Sensors and Materials, Vol. 17, No. 3 (2005) 125–137
MYU Tokyo

S & M 0592

Submicroliter-Volume Bulk-Micromachined Si-PMMA Thermal Cycler with a Multi-Stacked Dielectric Membrane

Dae-Sik Lee*, Se Ho Park, Haesik Yang,
Kwang-Hyo Chung and Hyeon-Bong Pyo

BioMEMS Team, ETRI, P.O. Box 106, Yuseong-Gu, Daejeon 305-350, Korea

(Received April 10, 2004; accepted December 7, 2004)

Key words: thermal cycler, Si, micromachining, multistacked, dielectric membrane

A micromachined submicroliter-volume thermal cycler with a multistacked dielectric membrane for the polymerase chain reaction (PCR) has been designed and fabricated; it has a fast thermal response and very low power consumption. The chip consists of a bulk-micromachined Si component and hot-embossed polymethyl methacrylate (PMMA) component. The Si component contains an integral microheater and temperature sensor on a thermally well-isolated membrane, while the PMMA component contains a 200 nL PCR chamber, valves and channels. The micro-hot membrane under the chamber is a silicon oxide/silicon nitride/silicon oxide (O/N/O) diaphragm with a thickness of 1.9 μm, which results in a very low thermal mass. In experiments, only 45 mW is required in the chip to heat the chamber to 92°C, the denaturing temperature of DNA. In addition, the heating and cooling rates are about 80°C/s and 60°C/s, respectively. From the fluorescence results from DNA stained with SYBR Green 1, we validated that the chip amplified the DNA from a vector clone that contained tumor suppressor gene BRCA 1 (127 base pairs at the 11th exon), after 30 thermal cycles each of 3 s, 5 s and 5 s at 92°C, 55°C and 72°C, respectively, in the chamber. As for the specificity of DNA products, because of the difficulty in analyzing results in the very small volume chips, we instead utilized the larger volume PCR products after cycling with the chip over the same sustaining temperatures but with much slower ramping rates (2.5–3.3°C/s) within about 20 min on a commercial PCR machine and confirmed the specificity with agarose gel electrophoresis. The proposed microchip can be used in the fully integrated, battery-powered instrument for DNA lab-on-a-chip applications.

*Corresponding author, e-mail address: dslee@etri.re.kr

1. Introduction

The polymerase chain reaction (PCR), a well-established in vitro method of amplifying nucleic acid molecules, is one of the most important technologies for genotyping and clinical diagnosis. Since repeated thermal cycling, involving denaturing (94°C), annealing (55°C), and extension (72°C), is necessary in PCR, the optimal design and fabrication of the temperature-controlling devices are very important for the speed of the thermal reaction and the efficiency of amplification.

For DNA lab-on-a-chip applications for real-time genotyping and diagnosis, a micro-thermal cycler with high speed and low reagent volume and with fluidic control of biological samples is important for real-time genotyping and diagnosis.[1] Various kinds of micromachined thermal cyclers have already been introduced.[2,3] However, recent interest has focused on submicroliter PCR amplification reactions because of advantages such as effectiveness, low cost, high throughput,[4–7] and the ability to integrate an amplification device and relevant components such as mixers, channels, valves and capillary gel electrophoresis.[2–3,5–6,8–9] In a typical microchip used for electrophoretic separation, the injection pathway can handle volumes less than 1 nL, thereby allowing the total volume for PCR to be decreased to the submicroliter range.[5,9] Oda *et al.* demonstrated the effectiveness of a 100 nL-scale PCR amplification reaction, in which the concentration of the primer-dimer was several orders of magnitude lower, while the signal of the PCR product was considerably higher, even within 10 PCR cycles, when compared with a traditional thermocycler.[4] In a submicroliter PCR, the heat ramping time in the chamber can be reduced in proportion to the square of the chamber dimension. Consequently, it is important to localize accurately and control the temperature in the nanoliter-scale chamber on the chip.[10] Furthermore, to develop a fully integrated battery-powered instrument for a lab-on-a-chip DNA analysis, microfluidic networks and power consumption must also be considered.

Microheaters are widely used in microsystems for local temperature regulation.[2,11–14] Portable applications also require microheaters to be self-governing in terms of electric power for as long as possible. Thus, some studies have dealt with dielectric membranes to insure good heat confinement on the surface of the membrane, thereby decreasing the power consumption and increasing the heat ramp rate. Indeed, the power consumption of a 1 μm-thick SiO_2 membrane is 75% less than that of a 1 μm-thick Si membrane at the same maximum temperature.[15]

In Si-based PCR microchips, a low pressure chemical vapor deposition (LPCVD), silicon-rich, low-stressed silicon nitride is usually employed as the heating membrane,[11–13] because of its stability, low thermal mass, good thermal isolation properties, and transparency for optical analysis of the reaction products. However, although this material is popular in typical micromachined applications based on its high etch resistance and low stress, it inhibits PCR reactions,[16] and, as a dielectric material, its film resistivity is adversely affected by excess silicon.[17] Furthermore, as for thermal isolation, the Northrup design[11] has a problem in that the walls of the chamber are made from the silicon wafer itself, which has high thermal conductivity. The heat flow path from the heater to the substrate passes through the fluid volume in the chamber, so the side walls of the chamber

can be much cooler than the silicon nitride membrane. Daniel *et al.* thermally isolated the PCR chamber from the rest of the silicon wafer using a silicon nitride membrane on the back side of the wafer and a thin mesh of silicon nitride on the front side.[12] Even though it enhanced the thermal response speed well to 60–90°C/s and also enhanced the maximum static heater power of 1.9 W at the highest operating temperature, those systems using a nitride dielectric membrane did not utilize microfluidics for lab-on-a-chip applications and required a larger heater power.

Therefore, this study utilized a unique dielectric multilayer O/N/O membrane for a submicroliter-volume thermal cycler employing standard CMOS processes, thereby producing a stable membrane that is compatible with PCR reactions and has both a high resistivity of 10^{16} Ω-cm and optical transparency. Plastics and polymers have also been used as materials for microfluidic structures because of their very good thermal isolation, low fabrication costs and ease of manufacturing.[18–20] We employed plastic to make fluidic networks.

Accordingly, in this study we designed, fabricated, and characterized a bulk-micromachined submicroliter-volume Si-PMMA thermal cycler with a multistacked dielectric membrane for use in a DNA lab-on-a-chip with a fast thermal response and very low power consumption.[21]

2. Materials and Methods

To obtain a rapid thermal response from the fluidic solutions in the chamber with reduced power consumption, silicon-based materials were used and the membrane structure was designed to integrate a microheater and resistance temperature detector (RTD) for precise thermal control of the fluid on the chip. When using dielectric layers as heating layers, the intrinsic stress in the membrane layers must also be considered, because intrinsic stress can occur in single or multilayer compositions and lead to membrane deformation or breakage. Because residual stresses are generally much larger than thermal stress, control of the residual stress in single and multilayer dielectric systems is crucial for membrane stability.[22]

For a multilayer system, a combination of silicon nitride and silicon oxide was employed. The intrinsic stress measurement for the dielectric layers was performed by measuring the deformation of a 5" silicon wafer after the deposition of a thin film. The results showed that the silicon oxide is compressive, whereas the silicon nitride is tensile. The right combination of silicon nitride and silicon oxide can lead to acceptable resultant residual stress and good surface passivation with PCR-compatibility. Therefore, stress-reduced stacked dielectric thin film layers composed of thermal and LPCVD SiO_2 (0.8 μm), LPCVD Si_3N_4 (0.3 μm), and LPCVD SiO_2 films (0.8 μm) were used, based on the equations in the following paragraphs. The physical properties of the stacked dielectric membrane design are shown in Table 1.[23]

The resultant residual stress, σ_r, of a stacked membrane (O/N/O) can be approximated by

$$\sigma_r = \frac{\sigma_{SiO_2} d_{SiO_2} + \sigma_{Si_3N_4} d_{Si_3N_4} + \sigma_{SiO_2'} d_{SiO_2'}}{d_{SiO_2} + d_{Si_3N_4} + d_{SiO_2'}} \quad (1)$$

Table 1
Physical properties of the stacked dielectric membranes.

Dielectric Film	Stress, σ (GPa)	Thickness, d (μm)	Young's modulus, E (Gpa)	Poisson ratio, υ
LPCVC SiO_2	–0.27	0.8	73	0.17
LPCVC Si_3N_4	1.2	0.3	323	0.25

$$\sigma_{SiO_2} = -0.27 + \left(E_{SiO_2} \times \alpha_{SiO_2}\Delta T\right) - \left(E_{SiO_2} / \nu \times \alpha_{SiO_2}\Delta T\right)$$
$$\sigma_{Si_3N_4} = 1.2 + \left(E_{Si_3N_4} \times \alpha_{Si_3N_4}\Delta T\right) - \left(E_{Si_3N_4} / \nu \times \alpha_{Si_3N_4}\Delta T\right) \quad (2)$$

Similarly, the resultant residual stress, σ_r, of a stacked membrane (N/O/N) can be approximated by

$$\sigma_r = \frac{\sigma_{Si_3N_4} d_{Si_3N_4} + \sigma_{SiO_2} d_{SiO_2} + \sigma_{Si_3N_4'} d_{Si_3N_4'}}{d_{Si_3N_4} + d_{SiO_2} + d_{Si_3N_4'}} \quad (3)$$

where, d, E, ν, α, d, and σ are the thickness, Young's modulus, Poisson ratio, thermal expansion coefficient, film thickness, and intrinsic stress, respectively, of the different membrane layers. Rossi *et al.* suggest an acceptable range for resultant residual stresses as –0.1 GPa<σ_r<0.1 GPa.[23]

Based on eq. (1) and using the film parameters for the three layers, the resultant stress was calculated to be –0.1 GPa<σ_r<0.1 GPa. The LPCVD Si_3N_4 layer in an O/N/O structure had the highest intrinsic stress values (1.2 GPa tensile), while the two oxide layers reduced the overall stress in the membrane. Likewise, the LPCVD SiO_2 layer in an N/O/N structure had an intrinsic stress value of –0.27 GPa compressive, while the two nitride layers reduced the overall stress of the membrane. According to eqs. (1) and (2), the σ range makes possible a wide range of silicon nitride and silicon oxide thicknesses through the PCR-temperature range from 27°C to 100°C as shown in Fig. 1. The acceptable stress region is shaded. In case of an N/O/N multilayer system, Fig. 1 can be translated into silicon nitride thickness (top plus bottom layers) versus silicon oxide thickness. Thus, the thickness of the O/N/O stacked membrane is designed to have an acceptable resultant residual stress (marked with an open circle in Fig. 1).

The thermal distribution in the microchamber was simulated based on water conditions using a CFD-ACE+ simulator (CFDRC, Alabama, USA) and simple geometry. The simulation analyzed one thermal step and the temperature distribution in a steady state. The simulation of thermal distribution data is shown in Fig. 2(a), Fig. 2(b), and Fig. 2(c). The steady state analysis showed good thermal isolation in the microchamber and a temperature distribution within ±1°C in the microchamber at a denaturing temperature of 92°C. There is, however, a small temperature drop at the edge of the microchamber. The thermal insulation of the membrane was fair in comparison to data in a recent paper.[24]

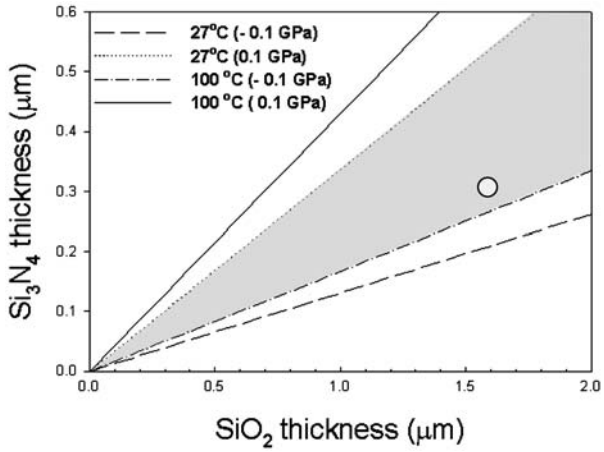

Fig. 1. Silicon nitride thickness vs silicon oxide thickness (top plus bottom layers) in an O/N/O multilayer system with $|\sigma|$<0.1 GPa. (It also can be translated into silicon nitride thickness (top plus bottom layers) versus silicon oxide thickness in an N/O/N multilayer system).

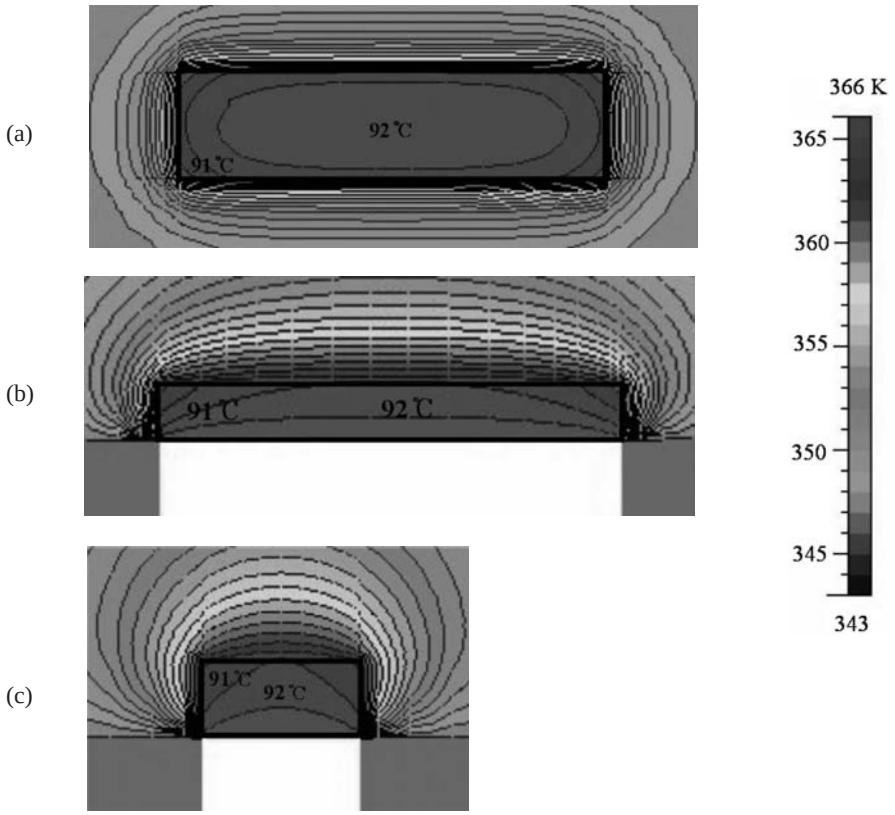

Fig. 2. Temperature distribution from within the microchamber at 92°C: (a) X-cut, (b) Y-cut, and (c) Z-cut sections (contour interval : 1°C).

Since it is reported that a PCR buffer with DNA has a much higher thermal conductivity than water,[25] when the reaction chamber is filled with the buffer solution, it is assumed that the temperature deviation between the upper and lower plate surface will be negligible.

The fabrication process was designed to be simple and suitable for mass production with semiconductor process-compatibility. The fabrication process for the thermal cycler involves creating a silicon bottom component and PMMA top component as shown in Fig. 3(a) and 3(b). A double-sided polished silicon (100) wafer, five inches in diameter and about 625 μm thick, was used as the substrate. After thermal oxidation of the wafer to grow silicon oxide (0.1 μm), SiO_2(0.7 μm)/Si_3N_4(0.3 μm)/SiO_2(0.4 μm) (O/N/O), deposited using the LPCVD system was used to create a stress-reduced heating membrane and etch mask on both sides of the wafer. First, the insulating layers on the bottom of the Si wafer, arranged for the heating membrane, were patterned by photolithography and etched down to the silicon using reactive ion etching (RIE). To fabricate the Pt thin film heater and resistance temperature detector (RTD) on top of the Si wafer, 0.3-μm-thick Pt was first deposited using an r.f. magnetron sputter with a 0.02-μm-thick Ti thin layer as an adhesion layer, then patterned by photolithography and etched using the RIE system. The alignment

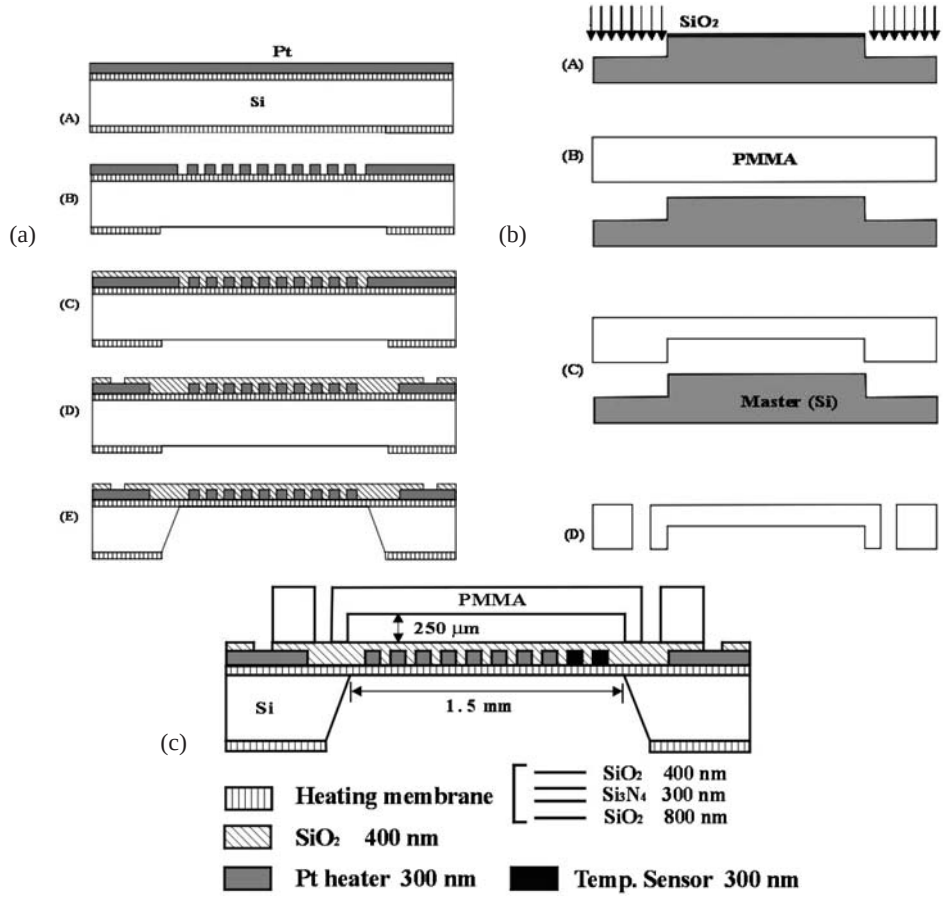

Fig. 3. Schematic of the major process steps in a thermal cycler process showing the following structures: (a) Si component, (b) PMMA cover component, and (c) cross-sectional view of the proposed submicroliter-volume bulk-micromachined thermal cycler.

of the patterns of the heater and RTD on top of the wafer with that of the heating membrane was accomplished by a bottom side alignment mask aligner (MA6, SussMicroTec co.). The silicon oxide (0.4 μm) was deposited using the LPCVD system on top of the wafer, then patterned by photolithography and dry etched using the RIE system on the platinum electrodes. The silicon oxide functions as both an electrical insulating and PCR-friendly layer and as a part of the stress-reduced membrane. To form the 1.9-μm-thick O/N/O heating diaphragm, the bottom of the silicon wafer was wet-etched in a KOH solution (26 wt.%, 85°C) through an entire wafer level using a custom-made etching manifold for sealing the top of the chip that allowed only the bottom of the silicon to be etched. Then the wafer was diced into discrete chips.

To fabricate the PMMA cover, the hot-embossing method was employed. A 625 μm-thick silicon (100) wafer was used as the master. To generate a master with microfluidic structures, 3-μm-thick silicon oxide was deposited on the wafer using PECVD, then patterned by photolithography and etched using RIE. Thereafter, deep reactive ion etching (DRIE) was utilized to make 250-μm-deep trenches (STS Co.). The structures on the silicon wafer were hot-embossed to the PMMA plate using a hot-embossing machine (HEX1, Jenoptiks). Then a 50-nm-thick silicon oxide layer was deposited on the plastic surface to enhance PCR-compatibility using an E-beam evaporator. The holes for the inlet and outlet were formed using a mechanical drill. Finally, the silicon component, including the heater and temperature sensor, and the PMMA component were bonded using a UV-curable adhesive. The cross-sectional view of the microchip is shown in Fig. 3(c) and the membrane section is highly exaggerated to show the structure. Photographs of the Si component, the PMMA cover component, and the resultant microthermal cycler are shown in Figs. 4(a), Fig. 4(b) and Fig. 4(c). The bulk-micromachined Si component integrates

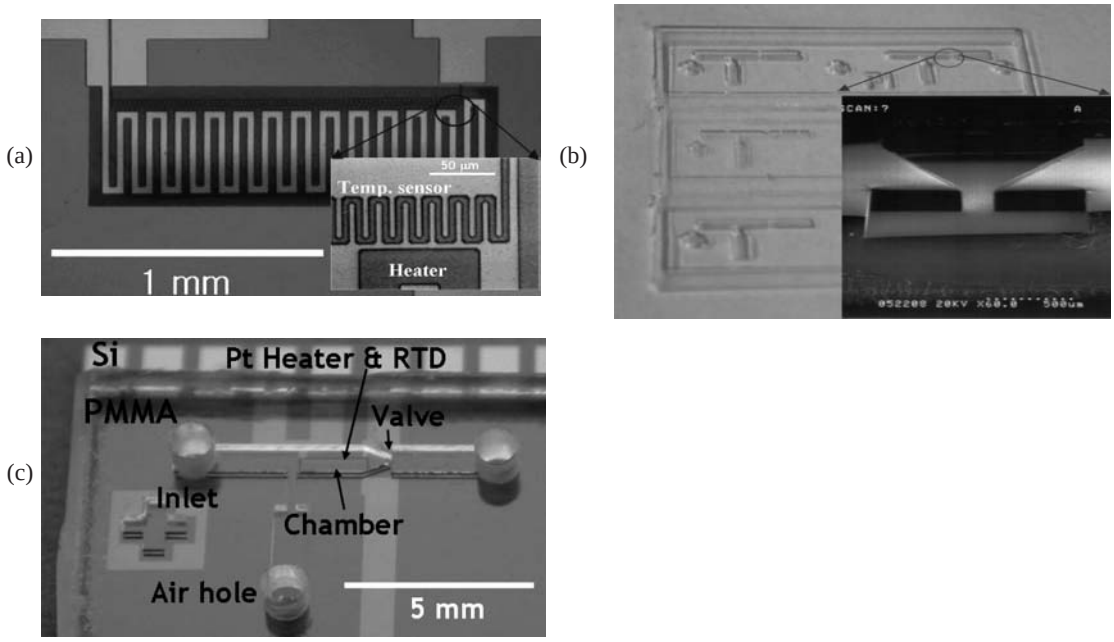

Fig. 4. Photographs of the micro-thermal cycler: (a) Si component integrated with a heater and a temperature sensor, (b) PMMA component with a chamber, a valve, channels, and holes, and (c) the fabricated submicroliter-volume bulk-micromachined thermal cycler.

with a platinum heater (line width 30 μm) and a platinum temperature sensor (line width 5 μm) in a serpentine for direct heat control in the microchamber. The PMMA component with a chamber, a valve, channels, and holes showed a steep edge profile. Furthermore, PMMA shows a good evaporation resistance even at a high DNA denaturation temperature (92°C). To meter the fluid in this thermal cycler, the sample injected from the inlet port flows into the reaction chamber after the air hole is closed. The sample fills the reaction chamber and the flow stops at the valve. Then the air pressure arrives at the hole for air injection, after the outlet port is blocked using silicone rubber. During the PCR amplification, all holes are closed using mineral oil or adhesive tape.

To perform a PCR using the chip, the PCR chambers are thermally cycled after the PCR chip is inserted into a custom-made pressure-fit electrical contact holder. The thermal cycling is controlled using the LabVIEW (National Instruments, Texas, USA) program without a proportional, integral, derivative (PID) module on a personal computer with a peripheral component interconnect (PCI) card. A precision digital multimeter (HP34401A) is used and the resistance across the RTD is collected and filtered using a low pass filter. The DAC output controlled by a personal computer with LabVIEW software controls the heater voltage applied through a DC power source (HP66312A). The schematic diagram for the chip PCR system setup is shown in Fig. 5. In order to view the PCR results, the fluorescence results from DNA bound SYBR Green 1 dyes were observed under a fluorescence microscope and gel electrophoresis was employed for specificity validation.

The thermocycling performance in a Si/PMMA thermal cycler was tested using a human cancer tumor-suppressing DNA sequence (BRCA 1, 127 base pairs at the 11th exon) that had been sampled from 1/30 diluted human blood, amplified using prepared primers, and then cloned into a Topo PCR 2.1 vector. The BRCA 1 gene primers prepared were: forward, 5'tgcttgtgaattttctgagacggatg 3', and reverse, 5' aacagaactaccctgatacttttctgga 3'; which amplified a 127 bp region of the gene. The reaction mixture was prepared in a 50 μl stock solution according to the following mixture: 2 × of an SYBR green dye, 5 μL PCR buffer, 2 mM dNTP, 2.5 units of Taq DNA polymerase, 2 mM $MgCl_2$, 0.4 μM of each of the two oligonucleotide primers, 15 ng of a cloned template, and sterile distilled water. The stock solution was divided into two parts. One part was used in the PCR microchip, while the other was used in a conventional thermocycler.

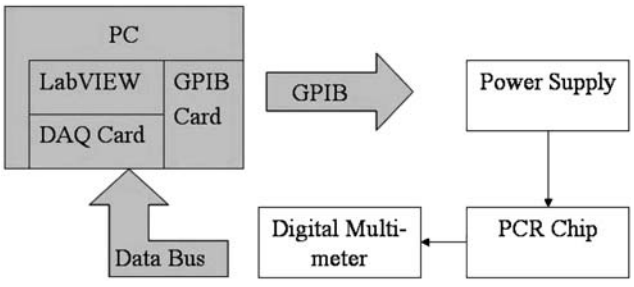

Fig. 5. Schematic diagram of the chip PCR system setup.

3. Results and Discussion

The resistance temperature detector was designed to enable fast thermal control and accurate temperature measurements. The location of the temperature sensors near the heater's lines on the topside of the membrane allowed for a direct thermal measurement in the microchamber. This also increased the accuracy of the measurement and reduced the time delay between the application of the temperature and its sensing. The resistance response as a function of temperature was extremely linear over the temperature range from 20°C to 100°C. Using this calibration line, the power consumption versus the temperature was measured in the microchamber solution as shown in Fig. 6. This figure highlights the extremely low electric power consumption that is critical for portable battery-powered applications, as only 45 mW was required for the denaturation step (92°C) and 23 mW for the annealing step (55°C), resulting in a good heater power coefficient of approximately 1.5°C/mW in terms of power consumption required.

Figure 7 shows the temperature profile as a function of time for complete profiles among the thermal cycles conducted in the micro chamber when using the calibration line and heater/RTD on the chip. With only resistive heating and passive cooling of the 200 nL chamber, a heating and cooling rate of over 80°C/s and over 60°C/s, respectively, was obtained. Thus, passive cooling was used to decrease the membrane temperature. With only passive cooling and resistive heating, even without a PID heat control module or a cooling fan, it was possible to reduce the overall thermal cycling time while reducing the operating power because of the high thermal ramp rates. Therefore, the low thermal mass of the microfabricated heating membrane, rapid heat transfer of the silicon, and high surface to volume ratio, approximately 13, of the 200 nL chamber facilitated fast heating and cooling and good PCR efficiency.

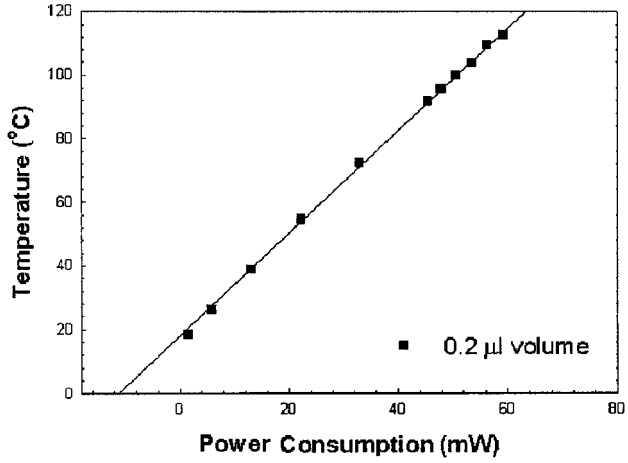

Fig. 6. Temperature versus power consumption required for the thermal cycler.

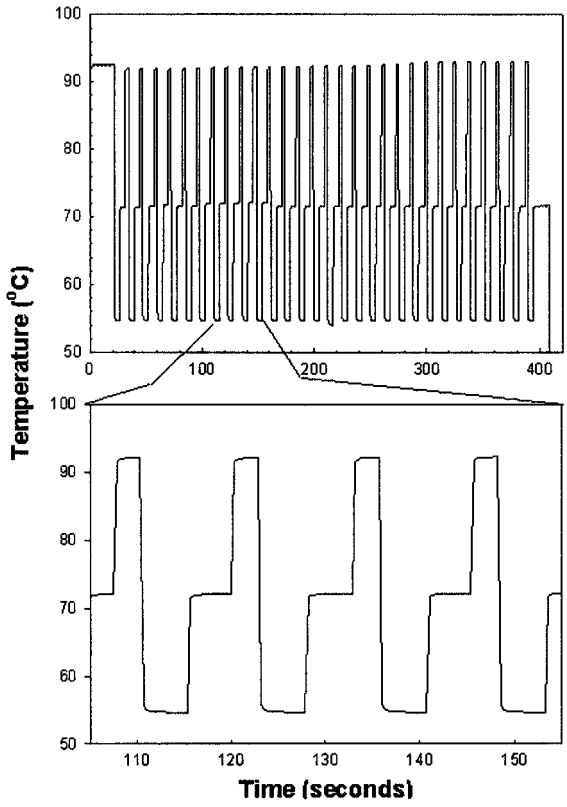

Fig. 7. Thermal cycling of the micro-thermal cycler with 0.2 µl fluid. Top: all 30 cycles of thermal cycling used in these experiments; 30 cycles are complete in 7 min. Bottom: an expanded view of 5 individual cycles, showing very fast heating and cooling obtained employing the micromachined membrane with heaters. Transition times were 0.25 s from 55°C to 72°C, 0.25 s from 72°C to 92°C, and 0.4 s from 92°C to 55°C.

In order to test DNA amplification in a thermal cycler, the microchamber on a chip was filled with approximately 200 nL of stock solution, including SYBR Green 1 dye, which binds to the minor groove of double-stranded DNA with a 800–1000-fold increase of fluorescence; several flushes of the mixture were utilized to remove any air bubbles that may have been trapped when filling the chamber. The chamber was then sealed using mineral oil to cover the inlet and outlet holes. The thermocycling conditions were as follows: 94°C for 10 s for the initial denaturation of the DNA, 30 cycles of 92°C (denaturing) for 3 s, 55°C (annealing) for 5 s, and 72°C (extension) for 5 s, followed by 10 s at 72°C for a final extension. The optimum annealing temperature was determined empirically according to the length and sequence of the primers used.[26] The total amplification time was approximately 7 min. Excitation of the dye-labeled DNA frag-

ments was achieved from a Hg UV source using a 488-nm light filter. The fluorescent PCR product from the microchip stained with SYBR Green 1 was collected through a fluorescence microscope and photographed using a charge-coupled device (CCD) with a band-pass filter centered at a wavelength of 560 nm.

Fluorescence photographs of the PCR results for a human cancer tumor-suppressing DNA sequence (BRCA 1) cloned into a Topo PCR 2.1 vector on the proposed micro-thermal cycler before and after 30 thermal cycles are shown in Fig. 8. The PCR products were observed immediately after the thermal cycles under a fluorescence microscope with an exposure time of 5.6 s. For fluorescence photographs of the PCR results for the BRCA 1 gene, SYBR Green 1 dye was added to the reaction mixture before PCR on the chip. An amplification was demonstrated after 30 thermal cycles of 3 s, 5 s, and 5 s at 92°C, 55°C and 72°C, respectively, within 7 min, which was at least 5–10 times faster than commercial instruments.

Finally, owing to the difficulty in gathering PCR results directly from the chip because of the small volume, the remainder of the PCR mixture was utilized in a specificity supporting experiment using a conventional thermocycler (Bio-Rad i-cycler). A Si chip containing 15 μL of the solution was run on a fast commercial thermocycler and cycled using the same temperatures, times, and number of cycles as in the experiments with the micro chip, except for the ramping rate set at the thermocycler (3.3°C/s when heating and 2.5°C/s when cooling). The collected samples were analyzed by running in a 2.5% agarose gel electrophoresis, which was stained with ethidium bromide after running. It takes approximately 20 min for 30 cycles on a commercial PCR machine. The PCR mixture in Si chip on the conventional thermocycler was loaded onto a 2.5% agarose for gel electrophoresis as shown in Fig. 9(a). As reference data, a gel electrophoresis of PCR products using the conventional amplifications in a conventional system is shown after 30 thermal cycles of 20 s, 30 s, and 12 s at 92°C, 55°C and 72°C, respectively, in Fig. 9(b). The data

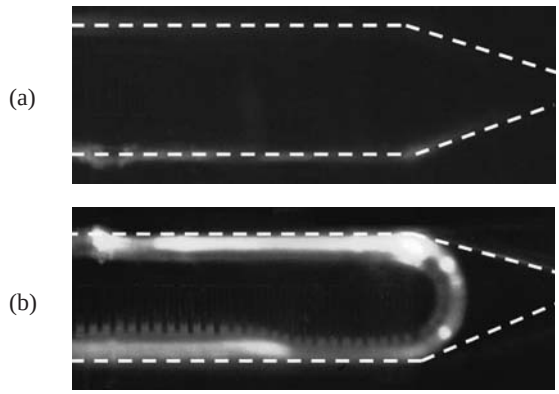

Fig. 8. Fluorescence photographs of PCR results for BRCA 1 gene dyed with SYBR Green 1: (a) before PCR and (b) after PCR on the chip (exposure time: 5.6 s; dotted line: chamber outline).

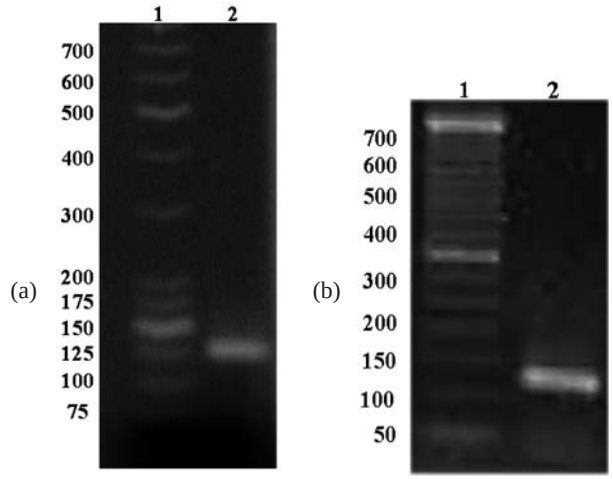

Fig. 9. Agarose gel electrophoresis of the PCR products amplified from BRCA 1 gene (a) on Si chip, and (b) PCR products from the conventional amplifications in a conventional system (lane 1: 25 bp marker, lane 2: PCR products).

show the same specificity and similar relative fluorescence intensity and demonstrate that the microchip using silicon has good performance with a steep reduction of process time and a small sample volume. The final amplified products revealed a DNA fragment with the expected size of 127 base pairs without any primer-dimer or nonspecifically-bound DNA.

4. Conclusions

A unique submicroliter-volume micromachined Si/PMMA thermal cycler with integrated Pt thermal sensors and a heater on a multistacked dielectric membrane for real-time temperature sensing and control for a DNA lab-on-a-chip was designed and fabricated. The multistacked dielectric membranes (combinations of silicon oxide and silicon nitride) deposited using a standard semiconductor process with LPCVD systems was employed as a stress-reduced thermally-isolated dielectric membrane, which makes possible a rapid thermal ramp speed and low power operation on the chip. With only a resistive heating and passive cooling scheme, a heating rate of over 80°C/s and a cooling rate of over 60°C/s were achieved experimentally. DNA amplification (a human cancer tumor-suppressing DNA sequence (BRCA 1) vector) in a 200 nL chamber was demonstrated after 30 thermal cycles within 7 min by fluorescence results from DNA bound with SYBR Green 1 dyes. As for the specificity of DNA products, because of difficulty in evaluating the PCR results in the very small volumes from the thermal cycler, we instead utilized the larger volume PCR products after cycling with the same sustaining temperatures as with the microchip, but with much slower ramping rates (3.3°C/s when rising, 2.5°C/s when cooling), for approximately 20 min on a commercial PCR machine. We verified the specificity to

BRCA 1 (127 base pairs) with agarose gel electrophoresis.
The proposed thermal cycler only required 45 mW to heat the reaction chamber to 92°C (corresponding to a heater power coefficient of ca. 1.5°C/mW), which is the denaturation temperature of DNA, and which is crucial to the development of a fully integrated and battery-powered lab-on-a-chip for a DNA analysis.

Acknowledgements

This work has been supported in large part by the Ministry of Information and Communication of Korea. The Si and PMMA device fabrication was performed at the ETRI CMOS fab. and MEMS Laboratory.

References

1 A. J. deMello: Lab Chip **1** (2001) 24.
2 L. J. Kricka and P. Wilding: Anal. Bioanal. Chem. **377** (2003) 820.
3 D. Erickson and D. Li: Analytica. Chimica. Acta. **507** (2004) 11.
4 R. P. Oda, M. A. Strausbauch, A. F. R. Huhmer, N. Borson, S.R. Jurrens, J. Craighead, P. J. Wettstein, B. Eckloff, B. Kline and J. P. Landers: Anal. Chem. **70** (1998) 4361.
5 E. T. Lagally, C. A. Emrich and R. A. Mathies: Lab Chip **1** (2001) 102.
6 M. A. Burns, B. N. Johnson, S. N. Brahmasandra, K. Handique, J. R. Webster, M. Krishnan, T. S. Sammarco, P. M. Man, D. Jones, D. Heldsinger, C. H. Mastrangelo and D. T. Burke: Science **282** (1998) 484.
7 O. Kalinina, I. Lebedeva, J. Brown and J. Silver: Nucleic Acids Res. **25** (1997) 1999.
8 R. H. Liu, J. Yang, R. Lenigk, J. Bonanno and P. Grodzinski: Anal. Chem. **76** (2004) 1824.
9 C. G. Koh, W. Tan, M. Zhao, A. J. Ricco and Z. H. Fan: Anal. Chem. **75** (2003) 4591.
10 S. D. Senturia: Microsystem Design (Kluwer Academic Publishers, Boston, 2001) Chap. 22.
11 M. A. Northrup, M. T. Ching, R. M. White and R. T. Watson: Transducers'93 Digest of Technical Papers (IEEE, Japan, 1993) 924.
12 J. H. Daniel, S. Iqbal, R. B. Millington, D. F. Moore, C. R. Lowe, D. L. Leslie, M. A. Lee and M. J. Pearce: Sensors and Actuators A **71** (1998) 81.
13 A. I. K. Lao, T. M. H. Lee, I. Hsing and N.Y. Ip: Sensors and Actuators A **84** (2000) 11.
14 H. Baltes, O. Paul and O. Brand: Proc. IEEE **86** (1998) 1660.
15 F. Udria and J. W. Gardner: Microelectron. J. **27** (1996) 449.
16 M. A. Shoffner, J. Cheng, G. E. Hvichia, L. J. Kricka and P. Wilding: Nucleic Acids Res. **24** (1996) 375.
17 E. S. Kim: Integrated microphone with CMOS Circuits on a Single Chip, PhD Thesis, Univ. of California, Berkeley (1990).
18 H. Becker and L. E. Locascio: Talanta **56** (2002) 267.
19 L. J. Kricka, P. Fortina, N. J. Panaro, P. Wilding, G. Alonso-Amigo and H. Becker: Lab Chip **2** (2002) 1.
20 J. Rossier, F. Reymond and P. E. Michel: Electrophoresis **23** (2002) 858.
21 D. -S. Lee, S. H. Park, H. Yang, T. H. Yoon, S. -J. Kim, H. Kim, Y. B. Shin, K. Kim and Y. T. Kim: Proceedings of the mTASí03 Symposium (IEEE, CA, USA, 2003) 187.
22 I. Simon, N. Barsan, M. Bauer and U. Weimar: Sensors and Actuators B **73** (2001) 1.
23 C. Rossi, P. Temple-Boye and D. Esteve: Sensors and Actuators A **64** (1998) 241.
24 J. El-Ali, I. R. Perch-Nielsen, C. R. Poulsen, D. D. Bang, P. Telleman and A. Wolff: Sensors and Actuators A **110** (2004) 3.
25 Y. C. Lin, C. C. Yang and M. Y. Huang: Sensors and Actuators B **71** (2000) 127.
26 S. H. Park, D.-S. Lee, H. Yang, K. Kim, S.-J. Kim, H. Pyo and C. Choi: Proceedings of the 6th KMEMS'04 Conference (KSS, Jeju, Korea, 2004).